Nanoscale Advances

COMMUNICATION

View Article Online
View Journal | View Issue

Cite this: *Nanoscale Adv.*, 2019, **1**, 965

Carbon nanotubes–elastomer actuator driven electrothermally by low-voltage†

Jae-Hun Jeong,[a] Tae Jin Mun,[a] Hyunsoo Kim,[a] Ji Hwan Moon,[a] Duck Weon Lee,[a] Ray H. Baughman[b] and Seon Jeong Kim *[a]

Received 11th September 2018
Accepted 5th December 2018

DOI: 10.1039/c8na00204e

rsc.li/nanoscale-advances

Electroactive polymers (EAPs) have attracted attention in many fields such as robotics, sensors devices and biomedical devices. However, the practical application of these actuators has still problems due to incomplete reversibility and high applied voltage. In order to overcome these problems, in this study, we have shown actuator based on phase transition that is consisted of the carbon nanotubes yarn infiltrated with the mixture of elastomer and methanol. Our electrothermally driven hybrid coiled yarn muscle provides a work capacity of 0.49 kJ kg^{-1} and a tensile contraction of 30.5% within ~3 s on an applied stress of 3.1 MPa at an applied DC voltage of 5 V. The maximum work capacity is under isobaric 23.4 MPa, which is 110 times that of typical mammalian skeletal muscles. This actuator may serve as a promising candidate for the practical use in soft robotics.

Artificial muscles that can convert electrical, thermal or chemical energy into mechanical energy for tensile contraction, torsional rotation or bending, have received considerable attention for their promising applications in exoskeletons, prosthetics devices and microfluidics.[1–4] Various types of materials, such as the piezoelectric ceramics,[5,6] electroactive polymers,[7–12] shape memory alloys[13] and shape memory polymers.[14–16] have been used as actuators that could be driven by external stimuli. Among them, electroactive polymers (EAPs) have received a considerable attention owing to the advantages of flexibility, lightness and low cost.[7,8] EAPs can be divided into two groups: ionic-EAPs and electronic-EAPs.[9] The electronic-EAPs, such as electrostatic, dielectric and liquid crystal elastomers, can be operated with a short response time and large strain. However, in order to actuate the electronic-EAPs, a high operating voltage is needed.[10–12] As a result,it is largely limited for many applications due to major safety concerns. To overcome the disadvantage of electronic EAPs, many researchers have considered phase change materials as the attractive alternative materials to conventional electromechanical actuators.[17–19] For example, Lima *et al.* introduced a single-plied coiled CNT yarn infiltrated with paraffin-based actuator.[17] This actuator provided the tensile actuation of over 5% by phase change at 32 V cm^{-1}. In addition, Zhou *et al.* reported carbon nanotubes (CNTs)/elastomer composite actuator, which could be driven by phase transition at low voltage (<100 V). The use of reversible liquid–vapour phase transition materials allows for a much larger expansion strain that can be obtained at low voltage.[12]

CNTs have been well known for attractive properties, such as low density, high tensile strength, high electrical conductivity and thermal properties that can be extended on a macroscopic scale based on a highly aligned structure of continuous CNTs fibers.[20–22] It has been reported that the formation of a coil structure with twisted CNT yarn can reversibly produce unique rotation and contraction due to volume change when driven by steam, solvent, light, current *etc.*[17,23,24] Among these actuation method, Joule heating has an advantage for practical application because of the easy temperature control and remote operation. In addition, the rapid thermal response of CNTs has become widespread in almost all heat-generating devices, such as electrothermal actuators.

In this communication, we fabricated a coiled yarn infiltrated with an elastomer–methanol composite, which was termed as the HCYM. The actuation of HCYM was caused by the gas pressure of vapourized methanol at low voltage. When using the HCYM, a work capacity of 0.49 kJ kg^{-1} and a maximum contraction of 30.5% can be achieved within ~3 s under an applied stress of 3.1 MPa at low input voltage (5 V). In addition, the HCYM actuator generated a short driving period and a higher shape recovery rate. A high mechanical work capacity of 0.85 kJ kg^{-1} was achieved under an applied stress of 23.4 MPa, which was 110 times higher than 7.7 J kg^{-1} of mammalian skeletal muscle.[25] The HCYM actuator had an excellent actuation and short driving period compared with electrothermal-based actuator.

[a]*Center for Self-powered Actuation, Department of Biomedical Engineering, Hanyang University, Seoul 04763, Korea. E-mail: sjk@hanyang.ac.kr*

[b]*The Alan G. MacDiarmid NanoTech Institute, University of Texas at Dallas, Richardson, Texas 75083, USA*

† Electronic supplementary information (ESI) available. See DOI: 10.1039/c8na00204e

The working mechanism for the electrothermally driven HCYM consisting of an infiltrating elastomer and methanol composite that was incorporated into a twisted and coiled CNT yarn has been shown in Fig. 1a. At power-on, the liquid of methanol converted to a vapour when the methanol in the elastomer reached the boiling temperature. Therefore, actuation occurred as the gas pressure increased inside the coiled yarn, which led to a volume expansion for the elastomer. When heating continued at a temperature slightly higher than the boiling point of methanol, further expansion occurred because of the increase in the elastomer pressure. As a result, the HCYM obtained excellent contraction. After the applied voltage was turned off, heat was lost by the air and the vapour became liquid methanol again and the actuator was restored to its initial state. Fig. 1b shows the scanning electron microscopy (SEM) image of the HCYM. The HCYM, having a diameter of around 220 μm, was fully coiled under a constant load of 7.8 MPa. The coiled structure provided a high actuation performance. In addition, the penetration of guest material into the neatly coiled CNT yarn improved the performance of the actuator, and effective distribution of guest materials was essential to achieve high contraction output and excellent stability. Fig. 1c and d show the different surface morphologies of neat CNT yarn and hybrid coiled yarn muscle, respectively. Before infiltration, the CNTs fiber bundles can be clearly observed. In contrast, as shown in Fig. 1d, a smooth region without interspace is observed on the surface of the hybrid coiled yarn muscle, which indicated that the CNTs fiber bundles were coated by elastomer–methanol composite material. These results show that the hybrid-coiled yarn muscle was uniformly filled with guest material to give an excellent actuation performance to the coiled hybrid yarn.

The used HCYM was prepared by twisting MWNT aerogel sheet drawn from a MWNT forest that was grown by chemical vapour deposition method. The resistance of the sample was greatly affected by the number of layers of CNTs sheet. Fig. S1† shows the relationship between resistance and the number of layers of CNTs sheet. Resistance decreased from 56.1 Ω cm^{-1} to 6.1 Ω cm^{-1} as the number of layers increased from 5 to 50. Accordingly, the sample resistance could be controlled by the CNTs layers. Moreover, in the case of 50 layers of CNTs, the temperature exceeded the boiling point of methanol, which was generated by the applied voltage. Therefore, the experiment was performed with 50 layers of CNTs sample.

The actuation performance of the HCYM was caused by the amount of methanol in the elastomer. Therefore, the effect of methanol amount in the elastomer on the contraction of the HCYM has been discussed and the result is shown in Fig. 2a. When the weight ratio of methanol to elastomer was 3 : 1, a maximum contraction of 30.5% was obtained compared with other samples. Besides, the presently used HCYM showed better actuation performance than the actuator of the coiled-CNT yarn infiltrated with paraffin that was electrothermally driven.[17] Unless otherwise noted herein, the coiled CNTs yarn infiltrated with a 3 : 1 weight ratio of methanol to elastomer was chosen and focused on this work. Fig. 2b shows the relationship between contraction, work capacity and the different twist insertion of initial CNT yarn. The increase in twisting of the initial yarn affected the amount of infiltrated elastomer–methanol composite and the actuation performance. When the twist insertion of initial yarn decreased, the low-inserted twist yarns provided a lot of internal void space in the yarn. Therefore, a relatively large amount of elastomer–methanol composite existed in the HCYM, which resulted in an excellent actuation performance. In contrast, when the twist insertion of the initial yarn increased, the highly twisted yarns offered less internal void space, which resulted in a relatively small amount of elastomer–methanol composite in the HCYM. As a result, the highly twisted yarn showed a low actuation performance. Based on these facts, the low-inserted twist yarn for the HCYM showed an excellent actuation performance and a work capacity up to 30.5% and 0.498 kJ kg^{-1}, respectively, whereas, the HCYM with highly twisted yarn provided a low performance with the contraction of 3.8% and a mechanical work capacity of 0.06 kJ kg^{-1} on the same stress. The reason for the difference in performance depending on the twist was due to the difference in the amount of elastomer–methanol composite in the HCYM. Experimentally, the HCYM with 500 turns per m could be made up to 92.4 wt% of elastomer–methanol composite, whereas the 3000 turns per m yarn was 81.9 wt%. Note in Fig. S2, ESI,† that the progressive increase in the layer number of CNT sheets was affected by the muscle contraction. The contraction of the HCYM progressively increased from 3.6% for 5 sheets CNTs to 30.5% for 50 sheets CNTs.

Fig. 3a shows the contraction actuation as function of time during five contraction/expansion cycles of the HCYM. Also,

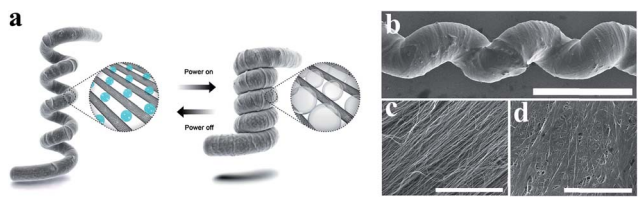

Fig. 1 The morphology of the HCYM. (a) Actuation mechanism of the HCYM driven by a DC voltage of 5 V. (b) SEM image of the HCYM. Scale bar, 500 μm. Higher-magnification SEM image of the surface morphology (c) before and (d) after the elastomer–methanol composite-infiltrated CNTs sheets. Scale bar, 5 μm.

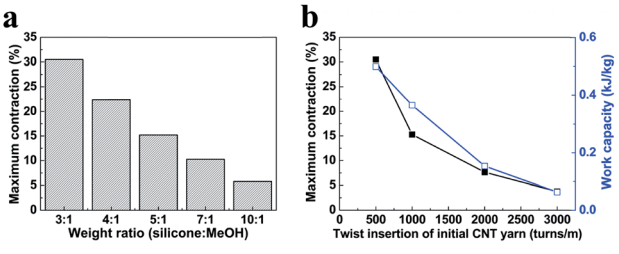

Fig. 2 The optimization of the HCYM. (a) The difference in elastomer weight ratio to methanol dependence of the contraction of the HCYM having similar coil index (~0.76) driven by a DC voltage of 5 V. (b) The twist insertion of initial CNT yarn dependent on the tensile actuation and work capacity of HCYM having a similar coil index (~0.76).

a fast response electrothermal actuator was obtained in this work. When the HCYM was heated electrothermally, the volume expansion, mainly caused by the phase transition of methanol from liquid state to vapour state, drove the contraction along the coil axis. At power-off, the HCYM was stretched until the original shape and length were substantially recovered due to phase transition from the vapour state to the liquid state. A contraction of 30.5% was obtained with an applied DC voltage of 5 V at an isobaric load of 3.1 MPa within 3 seconds. When the applied DC voltage of 5 V was turned off, the HCYM restored its initial length within 2 seconds (Movie S1 in the ESI†). When exposed to an external electrical stimulation a fast-response electrothermal actuator for the HCYM was obtained with its excellent tensile actuation and stability. Furthermore, the total contraction process took less time than an electrothermal-based actuator.[17,26] The stress dependence of contraction and specific work capacity for the HCYM was also electrothermally measured, as shown in Fig. 3b. Results revealed that an applied stress of 3.1 MPa had a maximum contraction of 30.5% and a specific work capacity of 0.49 kJ kg^{-1}, which was 63 times higher than that of typical mammalian skeletal muscles (7.7 J kg^{-1}).[25] The stroke decreased after applying stress below 3.1 MPa, which indicated that it was consistent with the proximity of adjacent coils impeding contraction. In addition, applying high stress reduced the stroke due to the lower Young's modulus of the yarn in the contraction state and the greater elastic elongation at higher loads in the initial state.[17]

At the stress of 23.4 MPa, the maximum specific work capacity was 0.85 kJ kg^{-1}, which is 110 times that of typical mammalian skeletal muscles. With the increase in DC voltage from 3 V to 8 V, the contraction actuations of the HCYM ranged from 3.5% to 39.3%, respectively, as shown in Fig. 3c. When DC voltage continued to increase, further expansion occurred. This is because the gas pressure increased in the elastomer–methanol composite, which led to the high contraction actuation of the HCYM. As shown in Fig. S3,† at high voltage (6 V and 8 V), although the high contraction actuation was achieved, the actuation performance of the HCYM remarkably decreased for 10 min. Conversely, at low voltage (4 V and 5 V), the actuation performance retained for 10 min. This is because methanol can stay trapped in the composite materials. Finally, Fig. 3d shows the reversibility of the actuation performance of the HCYM. The contraction was almost the same after a DC voltage of 5 V was applied during 50 cycles. By exposing the material to an air flow after the applied voltage was turned off, the temperature inside the coiled yarn decreased and the vapourized methanol became liquid again. This allowed the coil to elongate to its original length. The highly reversible actuation of HCYM can be obtained at low voltage.

Fig. 4 shows a novel application of the HCYM-based artificial muscle that can verify the applicability of the HCYM into the soft robot. The HCYM unit was designed, as shown in Fig. 4a and b, and applied it to the lever arm. To operate the lever arm, the commercial batteries (AAA, 6 V, ESI Fig. S4†) were used, resulting in a lever arm that could be smoothly moved by the HCYM actuator. When a stress of 23.4 MPa was applied to the actuator, a 10 g weight attached at the end could be lifted and

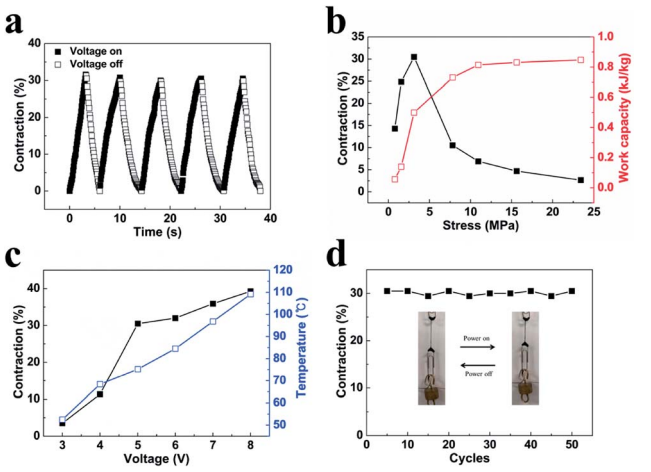

Fig. 3 Tensile contraction and work capacity of the HCYM. A 220 μm-diameter was used for the HCYM. (a) The contraction as a function of time during five cycles of the HCYM driven by a DC voltage of 5 V under an applied stress of 3.1 MPa. (b) The stress dependence of the steady-state tensile contraction and contractile work driven by a DC voltage of 5 V. (c) The contraction and temperature *versus* voltage for the HCYM with approximately a 3.4 cm length when different DC voltage was applied. (d) The contraction under an isobaric load of 3.1 MPa for 50 cycles with and without a DC voltage of 5 V. The inset shows the photographs of the HCYM with and without an applied DC voltage of 5 V.

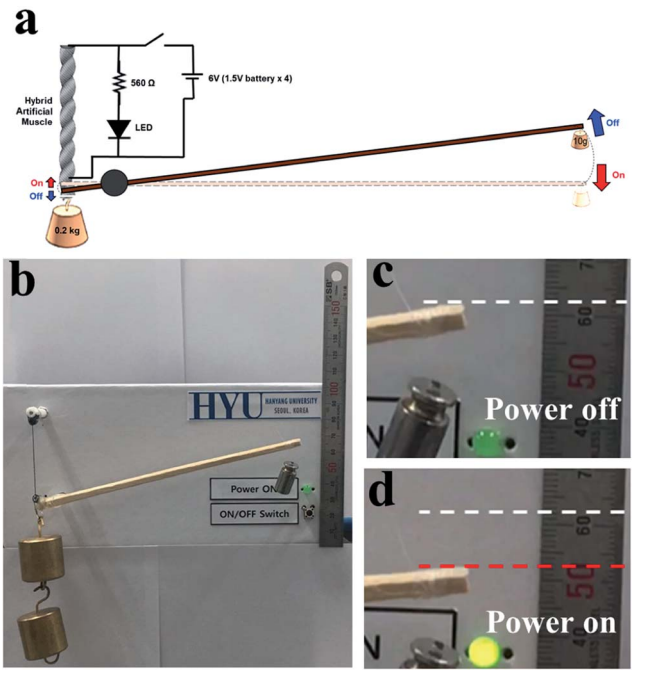

Fig. 4 Application of the HCYM actuator. A hybrid coiled yarn muscle (around 220 μm in diameter) was used to lift the pictured weight with and without an applied voltage. (a) Schematic of the circuit diagram based on electrothermal-driven contraction of the hybrid coiled yarn muscle. (b) The photograph shows the front of the HCYM. The lever arm lifted a 10 g load when the switch was turned (c) on and (d) off at 6 V using the commercial batteries (AAA type).

a ~1 cm could be moved with and without an applied voltage of 6 V, as shown in Fig. 4c and d and Movie S2.†

Conclusions

In summary, electrothermally-driven hybrid coiled CNTs infiltrated with a mixture of the methanol and elastomer composite (HCYM) were successfully fabricated. At power-on, the volume expansion, mainly caused by the phase transition of methanol from liquid state to vapour state, drove the contraction along the coil axis. When using the coiled CNTs yarn infiltrated with the methanol–elastomer composite (3 : 1 weight ratio) generated a high contraction of 30.5% and a work capacity of 0.49 kJ kg^{-1} were obtained under an isobaric stress of 3.1 MPa at an applied voltage of 5 V. The relationship between temperature and contraction proved to be advantageous in controlling the actuator and achieving a more accurate tensile actuation. The coiled composite yarn recovered its original length with a shape recovery ratio of nearly 100% at power-off. Also, shorter drive period (~3 s) and higher shape recovery were demonstrated in comparison with electrothermal-based actuator. Consequently, the HCYM has the advantages of easy-fabrication, lightweight, low applied voltage and high contraction. The HCYM might also be a promising candidate for its practical use in robotics, air vehicles and medical devices (*e.g.*, exoskeletons, micro-robots, prosthetics and microfluidics).

Conflicts of interest

There are no conflicts to declare.

Acknowledgements

This work was supported by the Creative Research Initiative Center for Self-powered Actuation in National Research Foundation of Korea. Support at the University of Texas at Dallas was provided by Air Force Office of Scientific Research grants FA9550-15-1-0089, and the Robert A. Welch Foundation grant AT-0029.

Notes and references

1 R. H. Baughman, C. X. Cui, A. A. Zakhidov, Z. Iqbal, J. N. Barisci, G. M. Spinks, G. G. Wallace, A. Mazzoldi, R. D. De and A. G. Rinzler, *Science*, 1999, **284**, 1340.
2 J. D. Madden, *Science*, 2007, **318**, 1094.
3 R. Pelrine, R. Kornbluh, Q. Pei and J. Joseph, *Science*, 2000, **287**, 836.
4 R. Pelrine, R. Kornbluh and G. Kofod, *Adv. Mater.*, 2000, **12**, 1223.
5 S. M. Parvasi, C. Xu, Q. Kong and G. Song, *Smart Mater. Struct.*, 2016, **25**, 055042.
6 S.-E. Park and T. R. Shrout, *J. Appl. Phys.*, 1997, **82**, 1804.
7 R. H. Baughman, *Synth. Met.*, 1996, **78**, 339.
8 Y. Bar-Cohen, *J. Spacecr. Rockets*, 2002, **39**, 822.
9 D. K. Seo, T. J. Kang, D. W. Kim and Y. H. Kim, *Nanotechnology*, 2012, **23**, 075501.
10 G. Wu, G. H. Li, T. Lan, Y. Hu, Q. W. Li, T. Zhang and W. Chen, *J. Mater. Chem. A*, 2014, **2**, 16836.
11 Q. Liu, L. Q. Liu, K. Xie, Y. N. Meng, H. P. Wu, G. R. Wang, Z. H. Dai, Z. X. Wei and Z. Zhang, *J. Mater. Chem. A*, 2015, **3**, 8380.
12 Z. Zhou, Q. Li, L. Chen, C. Liu and S. Fan, *J. Mater. Chem. B*, 2016, **4**, 1228.
13 S. Kalra, B. Bhattacharya and B. S. Munjal, *Smart Mater. Struct.*, 2017, **26**, 095015.
14 J. Li, T. Liu, S. Xia, Y. Pan, Z. Zheng, X. Ding and Y. Peng, *J. Mater. Chem.*, 2011, **21**, 12213.
15 J. S. Leng, W. M. Huang, X. Lan, Y. J. Liu and S. Y. Du, *Appl. Phys. Lett.*, 2008, **92**, 204101.
16 K. Ren, R. S. Bortolin and Q. M. Zhang, *Appl. Phys. Lett.*, 2016, **108**, 062901.
17 M. D. Lima, N. Li, M. J. de Andrade, S. Fang, J. Oh, G. M. Spinks, M. E. Kozlov, C. S. Haines, D. Suh, J. Foroughi, S. J. Kim, Y. Chen, T. Ware, M. K. Shin, L. D. Machado, A. F. Fonseca, J. D. W. Madden, W. E. Voit, D. S. Galvao and R. H. Baughman, *Science*, 2012, **338**, 928.
18 S. Ogden, L. Klintberg, G. Thornell, K. Hjort and R. Bodén, *Microfluid. Nanofluid.*, 2014, **17**, 53.
19 A. Miriyev, K. Stack and H. Lipson, *Nat. Commun.*, 2017, **8**, 596.
20 S. Ryu, Y. Lee, J. W. Hwang, S. Hong, C. Kim, T. G. Park, H. Lee and S. H. Hong, *Adv. Mater.*, 2011, **23**, 1971.
21 F. C. Meng, X. H. Zhang, R. Li, J. N. Zhao, X. H. Xuan, X. H. Wang, J. Y. Zou and Q. W. Li, *Adv. Mater.*, 2014, **26**, 2480.
22 L. Liu, W. Ma and Z. Zhang, *Small*, 2011, **7**, 1504.
23 P. N. Chen, Y. F. Xu, S. S. He, X. M. Sun, S. W. Pan, J. Deng, D. Y. Chen and H. S. Peng, *Nat. Nanotechnol.*, 2015, **10**, 1077.
24 J. A. Lee, N. Li, C. S. Haines, K. J. Kim, X. Lepro, R. Ovalle-Robles, S. J. Kim and R. H. Baughman, *Adv. Mater.*, 2017, **29**, 1700870.
25 J. D. W. Madden, N. A. Vandesteeg, P. A. Anquetil, P. G. A. Madden, A. Takshi, R. Z. Pytel, S. R. Lafontaine, P. A. Wieringa and I. W. Hunter, *IEEE J. Oceanic Eng.*, 2004, **29**, 706.
26 Y. Song, S. Zhou, K. Jin, J. Qiao, D. Li, C. Xu, D. Hu, J. Di, M. Li, Z. Zhang and Q. Li, *Nanoscale*, 2018, **10**, 4077.

